25th ABCM International Congress of Mechanical Engineering
October 20-25, 2019, Uberlândia, MG, Brazil

THE AERMEC TEST-RIGS FOR THE INVESTIGATIONS ON TURBINE BLADE FRICTION DAMPERS

Marcelo Braga dos Santos
FEMEC, Universidade Federal de Uberlândia
marcelo.bragadossantos@ufu.br

Chiara Gastaldi
DIMEAS, Politecnico di Torino
chiara.gastaldi@polito.it

Muzio M. Gola
Emeritus, DIMEAS, Politecnico di Torino
muzio.gola@polito.it

Tong Liu
Aerospace Res. Inst. Mat. Proc. Technol., Beijing
hitliutong@163.com

Abstract. *Under-platform dampers are commonly adopted in order to mitigate the resonant vibration of turbine blades. The need for reliable models to the design of under-platform dampers has led to a considerable amount of technical literature on under-platform damper modeling in the last three decades. The devices considered by this paper are "solid" dampers (as opposed to flexible "sheet" dampers), i.e. small but relatively rigid metal components which, during service, are loaded by centrifugal force against both lower parts of the platforms of two adjacent blades. When the relative movement between the blades increases such that slip between the damper and platform surfaces happens, blade vibration energy is dissipated through friction. The problem for the designer is to have the means to numerically simulate the damping mechanics, a task that can be satisfied by a simple numerical model, provided that reliable values of the contact parameters are available. Before the introduction of the first AERMEC damper test rig, the traditional experimental setup to evaluate the behavior of the damper under the platform was, and still is used, to measure the FRF blade (non-linear) after having incorporated the damper between two adjacent blades extracted from the real bladed disk. The effectiveness of the damper is then revealed by the difference in the response of the blade depending on the amount of radial force on the damper, the geometry of the damper, etc. It can be demonstrated, however, that parameter tuning is not unique, i.e., several combinations of contact parameters may produce the same response under a given set of external conditions. This does not produce contact parameters exportable to other conditions or to other blades. The first test bench designed and developed by the authors aimed to overcome this problem by directly measuring the forces applied by the damper to one of the platforms, together with the measurement of the kinematics of the platforms and the damper. Over time, the method was refined by introducing additional "local" measurements of contact tangential kinematics, and the determination of contact parameters has become increasingly reliable. The paper describes these improvements and illustrates how these connect with a numerical twin of the damper so that, despite the complexity of the system, it is possible to obtain a clearer understanding of the behaviour of the friction damper. Reliable knowledge is thus available that is useful in engineering applications where the amount of damping and the frequency shift are important design factors.*

Keywords: *Turbine blades, friction dampers, under platform dampers, friction measurements, mistuned blades.*

1. INTRODUCTION

Among the different devices used in the aerospace industries under-platform dampers are widely used in turbo engines to mitigate the blade vibration. Nevertheless, the damper behavior is not easy to simulate, and engineers have been working in order to improve the accuracy with which theoretical contact models predict the damper behavior. In laboratory simulators the damper is loaded by thin wires pulled by dead weights, a way to apply the equivalent of the centrifugal force, as indicated in Fig. 1.

Studies available in the literature rely on measuring the frequency response of blades under various sources of nonlinearity, where the FRF of the blade is the object of experimental observation. These are compared with those from a model: this is the case from the early pioneering 1980 studies (Griffin, 1980) through the decades down to the latest achievements (Pesaresi et al., 2017), (Gastaldi et al., 2018b), (Hüls et al., 2018), (Petrov, 2018), (Hartung et al., 2019).

Contact parameters are typically tuned so that the numerical FRF of a damped blade matches its experimental counterpart. This procedure is very debatable, as it is well known that there exist multiple combinations of the four normal and tangential contact stiffness values which produce a satisfactory match between a given experimental FRF and its numerical counterpart (Gastaldi and Gola, 2015).

Figures 1a,b serve a double purpose. On the one hand, Fig. 1a demonstrates what is anticipated in the introduction, that the tuning of parameters through FRF is underdetermined, namely that there are multiple combinations of contact parameters that produce a satisfactory match between given experimental FRF and its numerical counterpart (Gastaldi and Gola, 2015). On the other hand, they indicate, Fig. 6b, that the numerical model used is able to simulate its experimental twin very satisfactorily, provided that the contact parameters are correctly determined, even in one of the most difficult cases like that of a damper subject to liftoff.

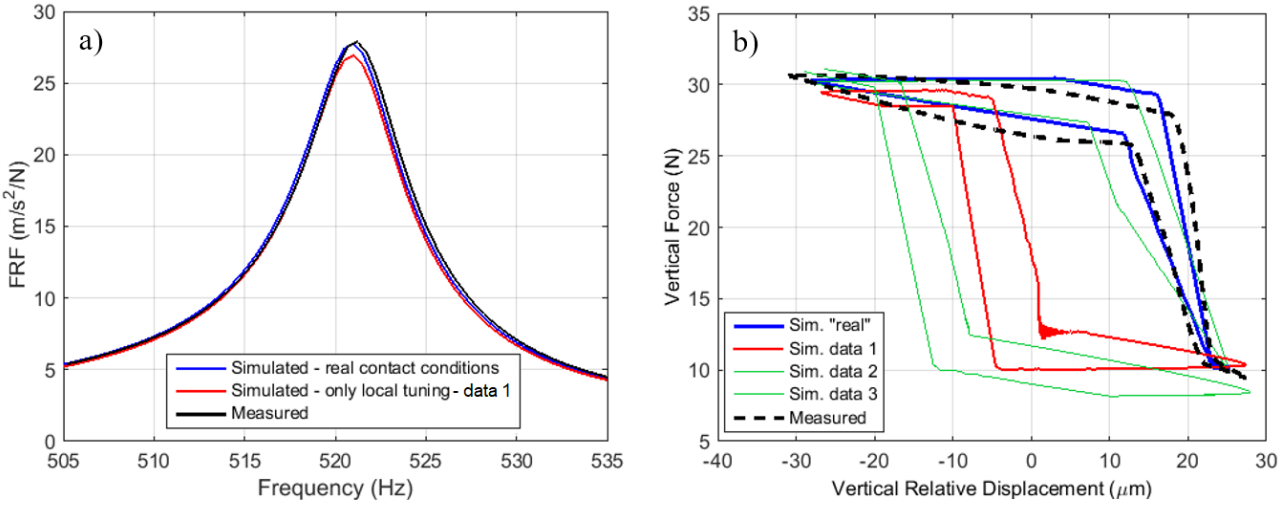

Figure 1. a): FRF of a blade on disk with dampers, interblade angle 0°, In-Phase, as measured and as simulated with two different combinations of contact parameters, b) In-Phase hysteresis cycles for a damper, as measured and as simulated with one correct and three incorrect parameter combinations.

What differentiates the AERMEC initial approach from all others in studies of damper mechanics, and their optimization, is the adoption of an original and innovative test rig named here "Piezo damper Rig I" (Gola et al., 2010).

The ultimate goal of these research activities is to provide the designer with a reliable tool for predicting the dynamic response of blade-damper systems. The logical and chronological development to obtain this result was the following. First of all, having a test-rig capable of providing accurate measurements of the forces and displacements that occur at the contact surfaces between the damper and the two adjacent platforms. Then develop measurement protocols, taking into account the characteristics of the transducers in use. Use experimental evidence to estimate contact parameters, to be fed into a dedicated numerical model of the damper. This model has been integrated into a non-linear FEM code that allows to simulate the dynamic vibration response of an entire bladed disk (Gastaldi et al. 2018a). Finally, a refinement concerned the effect of microslip on the damper damping capacity. Table 1 highlights the main details of such logical steps.

2. THE AERMEC TEST-RIGS

Fig. 2 and Table 2 summarize the main features of the three test rigs developed at AERMEC during the years. The "Piezo damper Rig I" was specially developed in 2007-2009 (Gola et al., 2010) to measure the in-plane forces transferred between the blade platforms through the under-platform damper as consequence of their relative displacement.

The "Piezo damper Rig I", as well as its later version "Piezo damper Rig II", is composed of two distinct parts each one representing a platform. One is static and accommodates the load cells, which measure the forces in two perpendicular directions; the other produces the in-plane motion, actuated by two piezoelectric stacks. The device reproduces any in-plane relative displacement between two adjacent platforms, be it In-Phase or Out-of-Phase, or any phase. At the same time, it measures both the relative motion between platforms and the forces they exchange.

The load measuring load cells are Dytran 1051V2, subject to a charge leakage, typically encountered in piezoelectric sensors, and thus unable to measure the static force component, thus requiring a lengthy load removal procedure (Gola et al., 2012) in order to get the total force value, which is necessary for equilibrium calculations.

In the first version "Rig I" the load cells on the right dummy platform are loaded through a "tripod" arranged parallel to the direction of the piezo actuators are pre-loaded by means of a wire pulled through a pulley and dead-weights (not visible) arrangement (Gola et al., 2010). The piezo actuators, hardly visible on the left and up, realize the platform motion through decoupling parallelograms. Fig. 3 summarizes the evolution of "Piezo damper Rig I" and the driving reasons.

Table 1. Developments on parameter tuning, nonlinear frequency response on real turbine blades

Development area	**Description**	**Main Papers**
Piezo Damper Test Rig development	Version 1: mechanical design and control software development to 2008, calibration and first measurements 2012.	Gola, Braga d. S., Liu 2010 Gola, Braga d. S., Liu 2012
	Version 2: 2013/14 upgrade of rig's dynamic performance.	Gola and Gastaldi, 2014
	Version 3: 2016 redesign of damper-platform contact.	Gola and Gastaldi, 2016, a
Measurement protocol	Version 1: 2008/12 development and refinements of the measurement protocol (kinematic and force-related quantities).	Gola, Braga d. S., Liu 2012 Gola and Liu, 2014
	Version 2: 2014 refinement of damper motion assessment.	Gola and Gastaldi, 2014
	Version 3: 2016 direct measurement of local tangential displacement at damper-platform contact	Gola and Gastaldi, 2016, b Botto et al., 2018
Contact parameter estimation	Piecewise I: 2010/13 three equal cylindrical contacts	Gola and Liu, 2014
	Piecewise II: 2013/14 one cylindrical and one flat contact	Gola and Gastaldi, 2014
	Random Sampling: 2015 automated DOE Latin Squares based	Gastaldi and Gola, 2015
	Piecewise III: 2016 direct assessment of tang. contact stiffness	Gastaldi and Gola, 2017
Numerical models	DTI: 2010/11 dyn. model of damper between two platforms	Gola and Liu, 2014
	DTI + HBM: 2014 comparison of. solution techniques	Gola and Gastaldi, 2014
	Dynamic model of blades-dampers system	Gastaldi et al. 2018 a-b
Microslip contact param. estimation	Introduction of microslip models into the platform-damper contacts, validation against microslip experimental data	Gastaldi and Gola, 2016 c Li et al., 2018

Table 2. Main features of the three damper-dedicated test rigs developed at AERMEC

	Piezo damper rig I	**Resonant blade rig**	**Piezo damper rig II**
Scope	Stand-alone damper behaviour	Damper coupled with a blade (real or dummy)	Stand-alone damper behaviour
Input motion	In plane motion, range ~ 70 μm	Constrained by blade-platform kinematics	In plane motion, range ~ 100 μm
Response of blade	×	✓	×
Damper contact forces	✓	✓	✓
Damper/Platform kinem.	✓	✓	✓
Frequency range	Up to 150 Hz	FRF up to 4500 Hz, damper up to 1500 Hz	Up to 500 Hz
Flat contact pressure *	Up to 2 MPa	Up to 6 MPa	Up to 6 MPa
Temperature	Room temperature	Room temperature	Room temperature

An improvement introduced in "Resonant blade rig", designed in 2014 (Botto et al., 2018), Fig. 1, was to replace these load cells with KISTLER 9323AA charge piezo load cells with "very small" leakage, (0.1 mN/sec as measured by the authors) which do not filter out the static component of the measured force. Certainly, this rig differs also in the way in which the vibration of the platform is generated, that is, by exciting a blade, both real and dummy, in resonance. The reasons for this choice and its results are not discussed here.

The latest version of the "Piezo + Damper Rig II" adopts the new load cells on the force measurement side, while on the movement generation side it adopts a single piezo actuator of higher performance, suitable to provide higher frequencies and forces (Gastaldi and Gola, 2019).

To the authors' knowledge, there are some documented cases in the literature of measuring the rotation of the damper during the vibration of the blades, (Firrone, 2009), (Pesaresi et al., 2017) but there are none of simultaneous measurement of the forces exchanged on the damper.

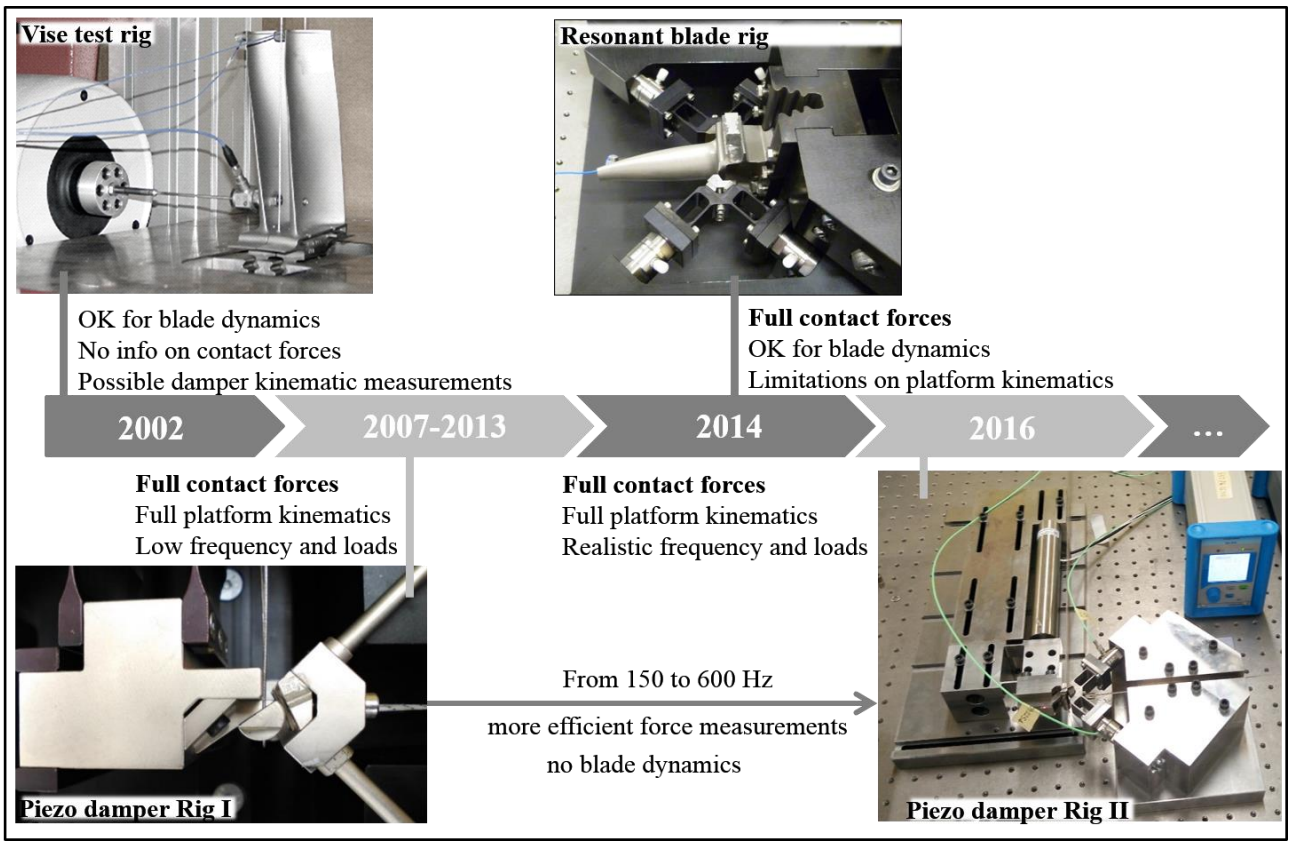

Figure 2. The time evolution of damper test-rigs at AERMEC Lab.

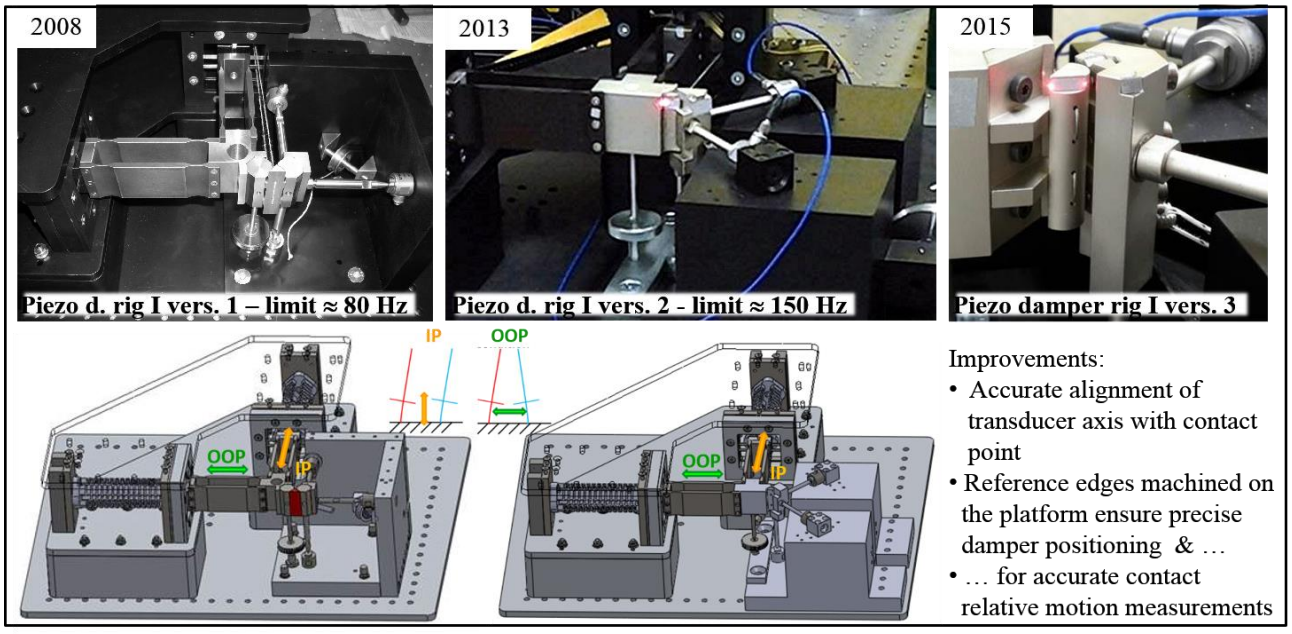

Figure 3. The time evolution of “Piezo damper Rig I”: main improvements to upgrade operating frequency, contact pressures, accuracy, and to allow laser measurement of both the damper’s absolute motion and of the relative tangential motion at the contact with the platform. Assessment of the damper mechanical behaviour

The first damper tested on Piezo damper Rig I was the three-bosses damper shown in Fig. 4, under an "equivalent centrifugal" load of 45 N, at frequencies 5, 40 and 80 Hz and nominal platform displacements 20, 40 and 60 μm.

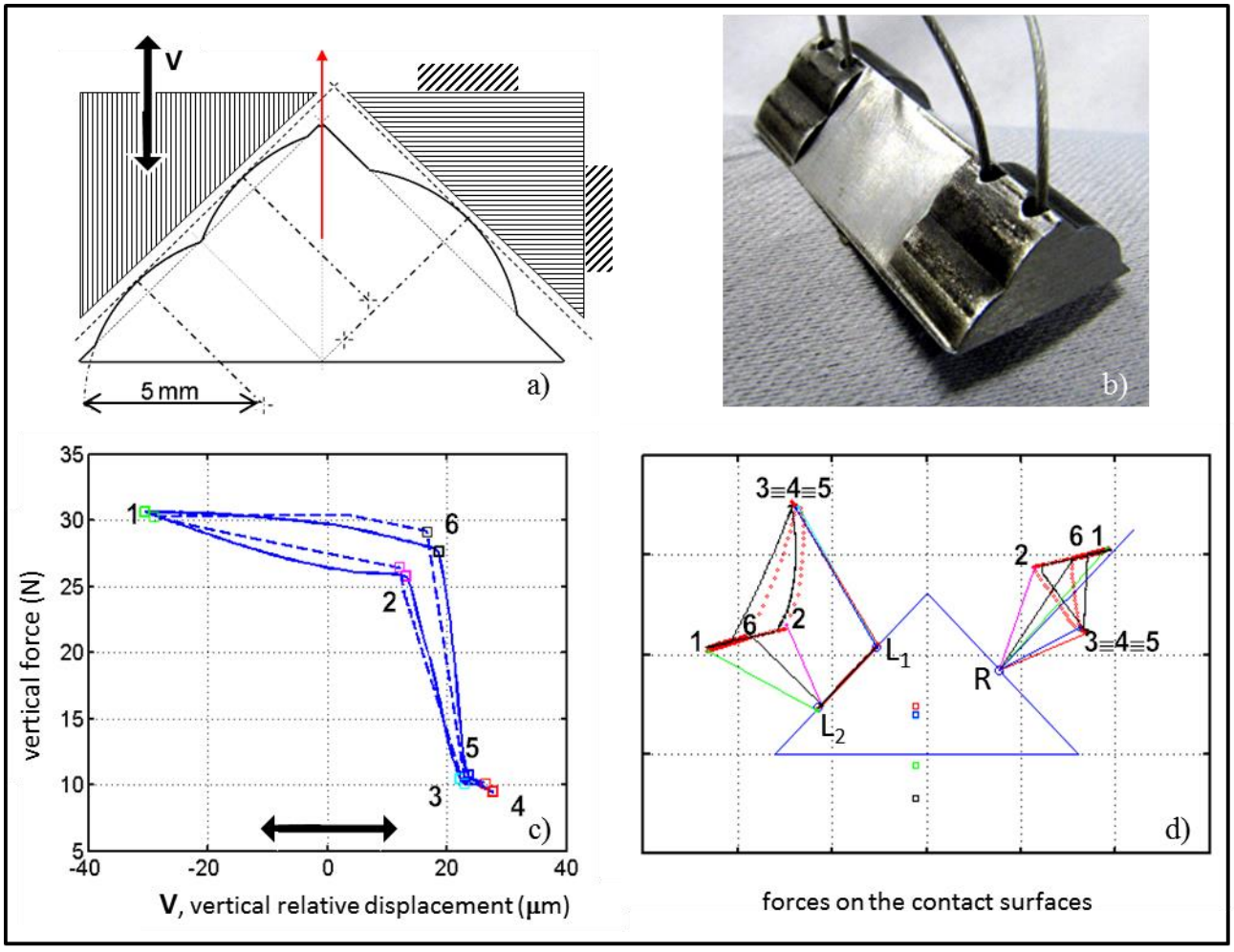

Figure 4. Three-boss damper: a) damper shape and dimension, b) damper picture, c) platform-to-platform hysteresis cycle, In-Phase i.e. vertical relative motion of platforms, d) experimental force vectors on the lateral damper surfaces

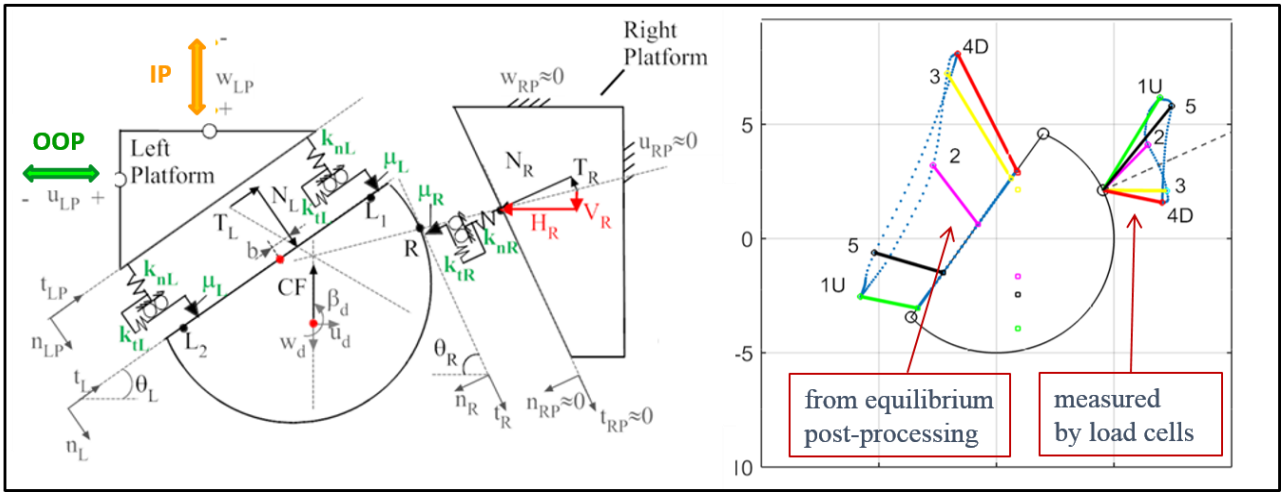

Figure 5. Flat-curved damper: left: scheme of the numerical model, right: forces on damper as assessed experimentally

Fig. 4 schematically shows that damper, with its cylindrical Hertzian contact lines, a vertical force-displacement cycle and a representation of experimentally obtained force. As explained in (Gola et al., 2012), (Liu, 2013), (Gola and Liu, 2014b) under those particular experimental conditions this damper was undergoing liftoff: a practice not recommended

for damping efficiency, however methodologically useful in the first development phase because at the ends of the cycle the force on the left side should fall exactly on points L1 and L2. Like Fig. 4d shows that actually happened (Gola et al., 2012), (Gola and Liu, 2014b). Providing confidence that the whole process of measurement and data elaboration was reliable.

While the three-boss damper was meant to be a purely laboratory damper, indeed a most challenging one to the experimenter being prone to liftoff, in the second development phase the dampers used during the following investigations were of the realistic "flat-curved" type shown in Fig. 5 machined from 10 mm diameter cylinder, in a number of versions exploring the angles of inclination on the two sides and the depth of the flattening on the left side. For all tested dampers, however, a numerical twin of the damper between the test-rig platforms, as in the example of Fig. 5a, was used to the purpose of calculating simulated cycles thus allowing the determination of contact parameters, see Tab. 1 by fitting them to the experimental ones (Gola and Gastaldi, 2014a), (Gola and Liu, 2014b), (Gastaldi and Gola, 2015), (Gastaldi, 2017).

During the second development phase, experience suggested to gradually add incremental and essential improvements to the platform and damper, such as illustrated graphically in Fig. 6,7. Moreover, replaceable platform inserts (Fig. 7b shows the left platform insert) were introduced in order to accommodate different materials and geometries, Fig. 7.

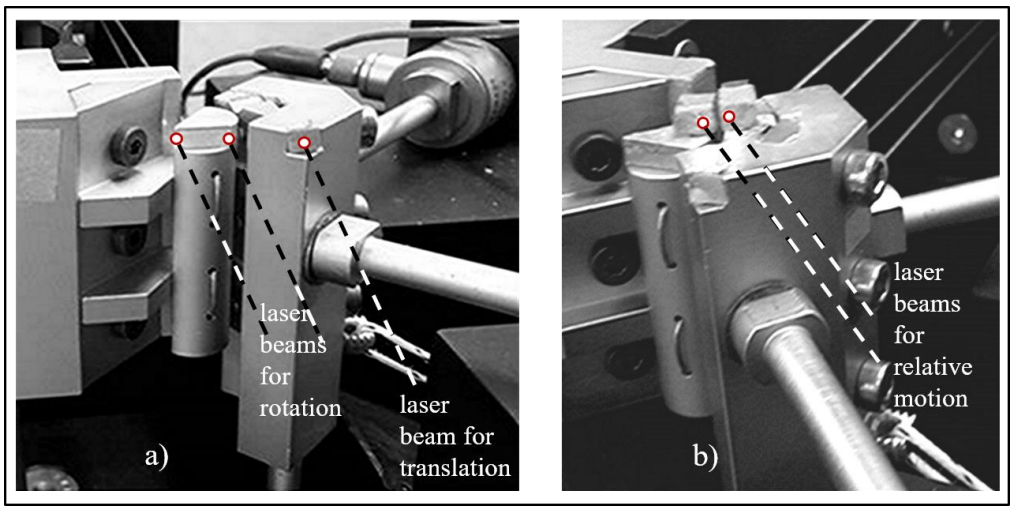

- recesses to accommodate laser reflecting surfaces (Fig. 6a)
- reference marks machined on the platform ensure precise damper positioning and aligning (Fig. 7a)
- localized damper-to-platform contacts, for higher contact pressure and more uniform distribution (Fig. 7b)

Figure 6. a A curved-flat damper (loops of pulling wires visible on its bottom) between the platform as at 2015. Laser beams are measuring the damper's rotation. (b) Laser beams are measuring the relative tangential motion at the contact between damper and right platform.

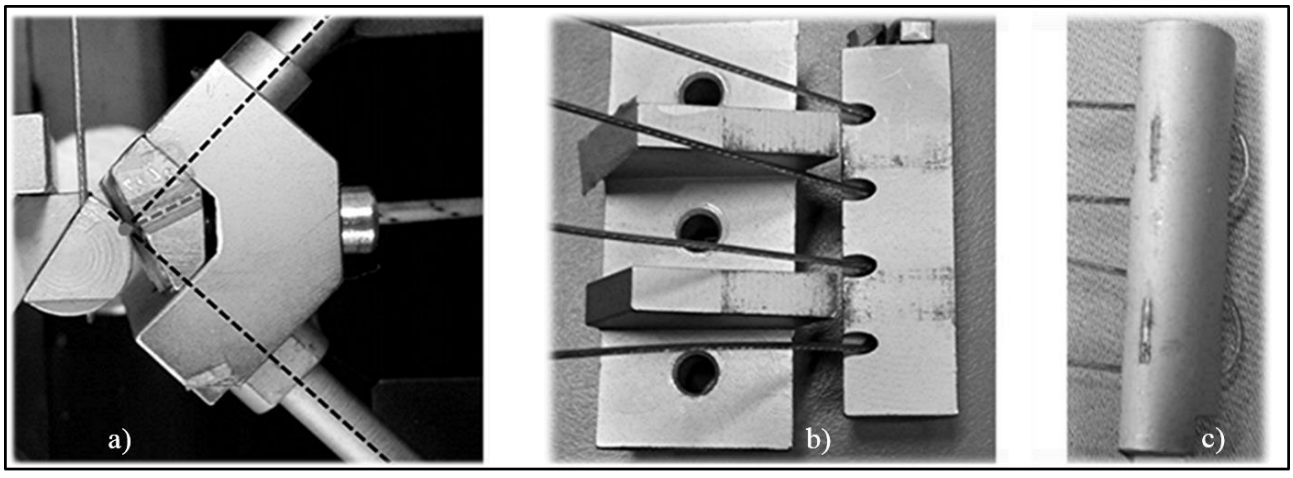

Figure 7. a) the cylinder-platform contact point aligned on the intersection of force transducer axes, b) the left platform (flat-on-flat contact) in the form of "ribs" to localize contact surfaces, guarantee contact uniformity, allow higher contact pressures, c) wear marks on the corresponding right damper surface, on the corresponding right platform ribs.

Such improvements made it possible to obtain the measurement performance summarized in Table 3 for the parameters that are either directly measured or derived through equilibrium and kinematic calculations, together with the standard deviations of their estimates.

Table 3. Parameters observed and derived on the basis of damper equilibrium and kinematics – Piezo damper rig I

	Estimated parameters	Standard deviation values	
OBSERVED	• Right Contact Forces	• 3% (≈0.5 N)	forces
	• Platforms relative displacement. • Damper rotation • Damper vertical displacement. • Damper tangential relative displacement. at the contact	• 0.08 μm • 5% (≈0.6·10-4 rad) • 0.08 μm • 0.08 μm	kinematics
DERIVED	• Left Contact Forces + force application point • T/N force ratios	• 3-5% (≈0.7-0.9 N), 0.5 mm • <4% (right), <9% (left)	forces
	• Damper tangential relative displacement. at the contact	• 5% (≈0.5 μm)	kinematics

In addition, during the second development phase a check was carried out on the accuracy of the damper kinematics measurement and processing procedures similarly to what had already been done for forces, see Fig. 4d. Indeed, a quite convincing proof of the accuracy of the rig, and of the reliability of the various procedures developed to treat the kinematic data is provided by the following cross comparison of two distinct sources for the same displacement. As described in (Gola and Liu, 2014), by pointing two laser beams on the bottom of the damper, Fig. 8a, its rotation is directly measured together its displacement along the orthogonal to the damper's flat bottom. . The damper's absolute displacement comes from one damper motion and the simultaneous right platform motion, which cannot be assumed to be zero due to its elastic constraints.

The tangential relative displacement $\mathbf{t_{RD}\text{-}t_{RP}}$ is then mathematically deduced given the tangential constraint condition at the contact between damper and platforms, as illustrated in Fig. 8b. In Fig. 8c, the tangential relative motion due to pure slip or to tangential elasticity is separated from the effect of pure rolling.

However, the same $\mathbf{t_{RD}\text{-}t_{RP}}$ displacement is directly observed by pointing two laser beams at the contact location, Fig. 6b and 9, as detailed in (Gastaldi, 2017). Figure 9 compares the observed vs. derived displacements, and shows that they indeed do match extremely well.

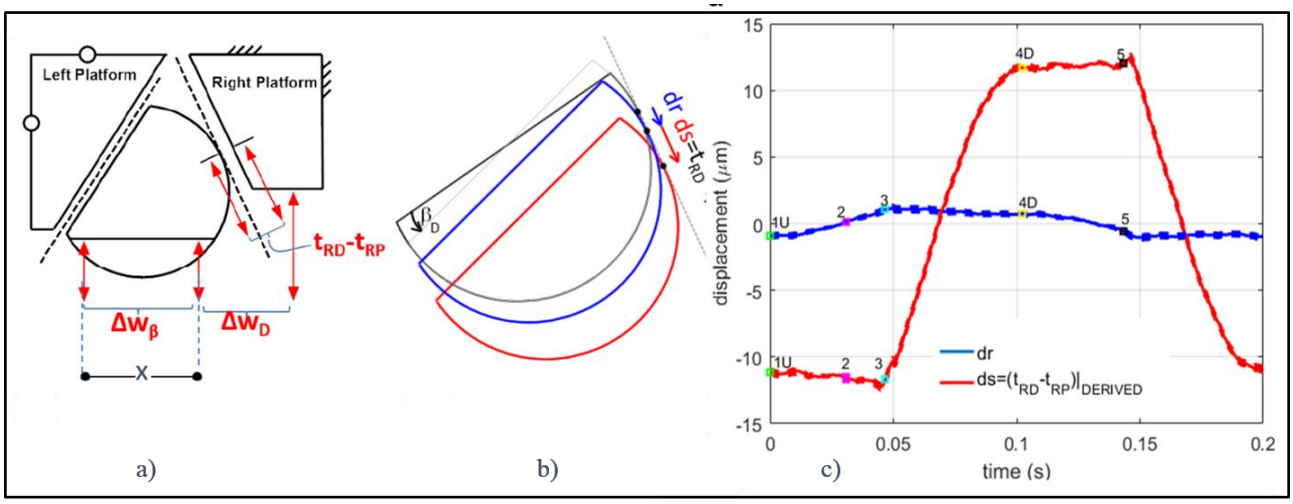

Figure 8. a) Laser measurement points for damper motion, absolute (Δw) and relative to the right platform ($\mathbf{t_{RD}\text{-}t_{RP}}$) b) Rolling and sliding scheme, c) Contact point motion on platform due to rolling (**dr**) and damper tangential displacement due to spring/sliding ($\mathbf{ds= t_{RD}\text{-}t_{RP}}$)

The relative damper-platform tangential motion can then be related to the corresponding tangential contact force component in the so-called platform-to-damper local hysteresis cycle. Figure 10a and Fig. 10b show the flat-on-flat and cylinder-on-flat local hysteresis cycles respectively, measured on a curved-flat damper on the Piezo Damper Rig I vers. 3, under an equivalent "centrifugal" load of 45 N, at 5 Hz and a nominal platform displacement of 50 μm.

The slopes of the local hysteresis cycles can be used to estimate the tangential contact stiffness values at the two contacts, k_{tL} and k_{tR} : these two calibration parameters are then fed into the numerical model, Fig. 5.

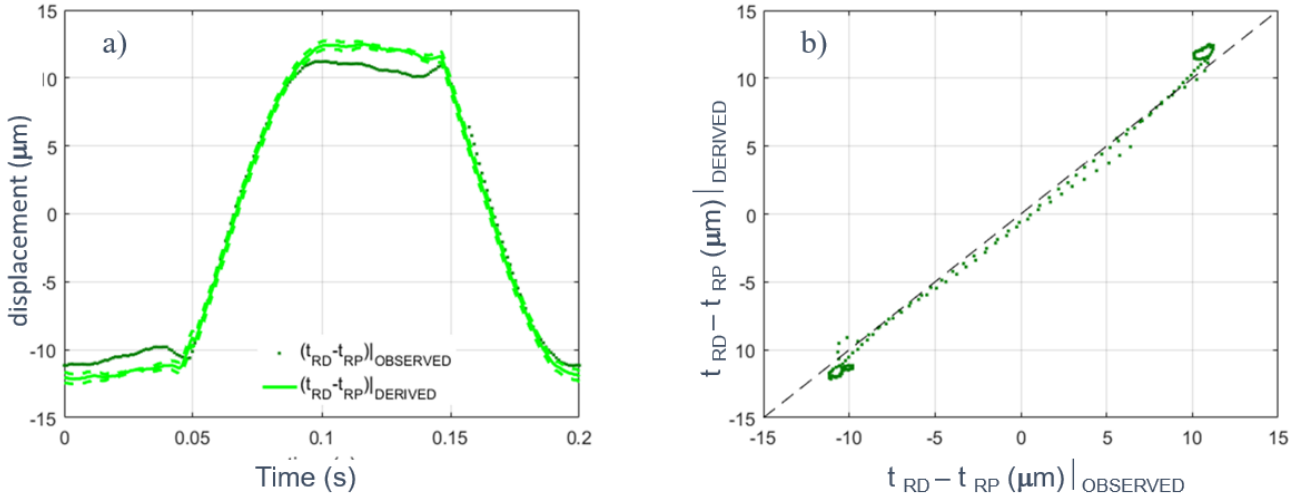

Figure 9. a) Relative tangential displacements **ds= t_{RD}-t_{RP}** both directly observed and derived
b) Comparison of kinematically derived **ds= t_{RD}-t_{RP}** with its observed counterpart.

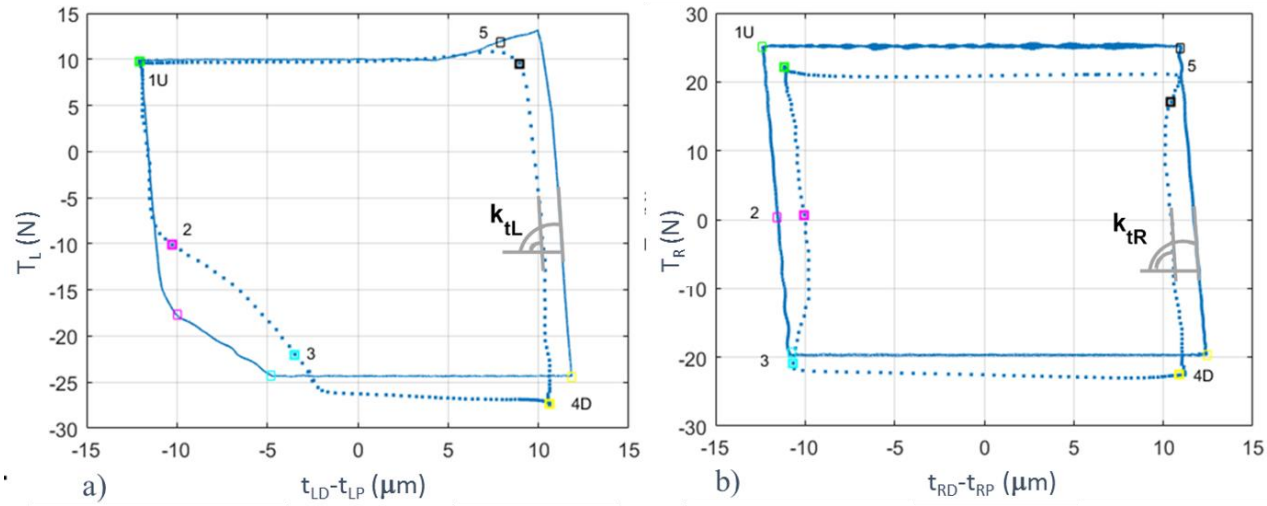

Figure 10. a) Left (flat-on-flat) local platform-to-damper hysteresis cycle measured (dotted) and simulated (solid)
b) Right (cyl-on-flat) local platform-to-damper hysteresis cycle measured (dotted) and simulated (solid).

Another relevant diagram is the platform-to-platform hysteresis cycle, already shown in the case of the three-boss damper in Fig. 1b and Fig. 4c. In it, the relative platform motion, directly measured by means of the differential, is related to the corresponding component of the right (or left) contact force. In case of In-phase motion the relative displacement between the platforms is purely vertical, therefore the vertical component of the contact force is chosen.

One notable property of this diagram is its capability of representing the overall damper behavior. The area inside the cycle represents the global dissipated energy and its shape gives an indication on the damper behavior. The three-boss damper, prone to lift-off, sports an irregular banana-shape hysteresis with a limited inner area (see Fig. 4c). The curved-flat damper from Fig. 5, on the other hand, does not roll. As a result, the shape of the platform-to-platform hysteresis cycle in Fig. 11a is regular, typical of a highly efficient stick-slip pattern, compatible with the considerable imposed relative platform motion.

A further confirmation of the soundness of the experimental evidence can be obtained by computing the total dissipated energy using two alternative methods. As mentioned above, the area of the platform-to-platform hysteresis cycle represents the overall energy dissipated by the damper over one period of vibration, it amounts to 1670 N·μm in the Fig. 11a case. The same result can be obtained through the sum of the areas of the corresponding platform-to-damper hysteresis (cycles in Fig. 10), in this case 1595 N·μm. A 4 % discrepancy is perfectly acceptable, especially considering that the comparison has been performed using the results from three independent measurements.

Another relevant diagram is shown: the tangential-to-normal force ratio at the two contacts is plotted as a function of time, as in Fig. 11b. These ratios are used to determine contact states at a given instant in time (i.e. gross slip if ratio is constant, stick if ratio is varying in time) and, if gross slip is present, to estimate friction coefficient values at the two interfaces. The friction coefficient values are an essential parameter of the numerical model in Fig. 5a.

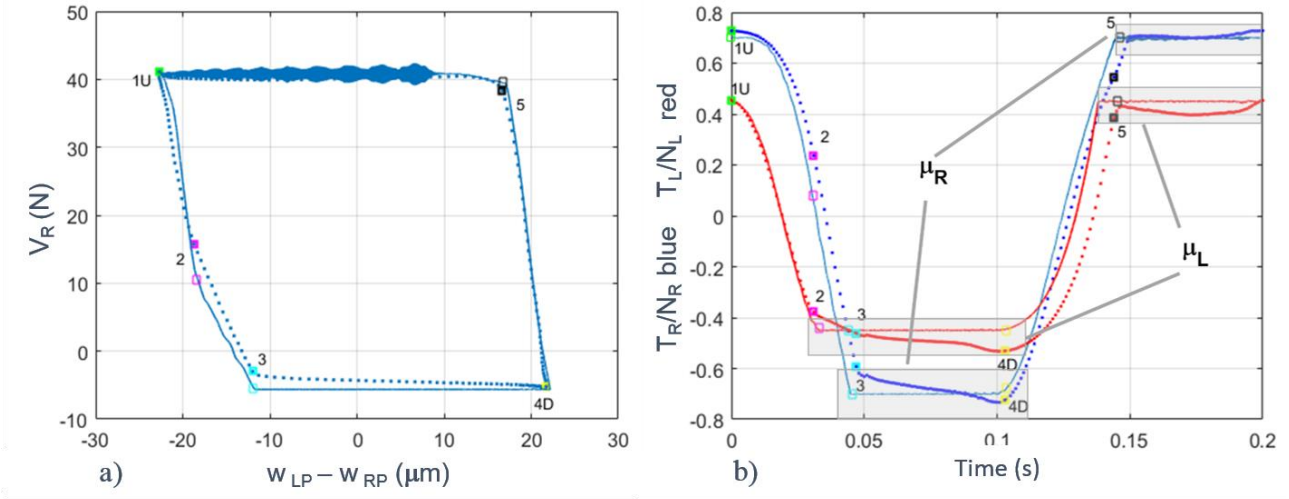

Figure 11. (a) Platform-to-platform hysteresis cycle, measured (dotted) and simulated (solid).
(b) Tangential-over-normal force ratio over a period of vibration, measured (dotted) and simulated (solid).

The centrifugal load and frequency limitation of the Piezo Damper Rig I have been overcome by the piezo Damper Rig II. Contact parameters such as the tangential contact stiffness values ktL and ktR are influenced by the contact pressure, (Gastaldi and Gola, 2019). The comparison of both platform-to-platform and local hysteresis cycles recorded on the same damper at different frequencies (Fig. 12) demonstrates that, at least in the [10-300] Hz range, frequency does not influence neither the damper behavior nor the contact parameter values.

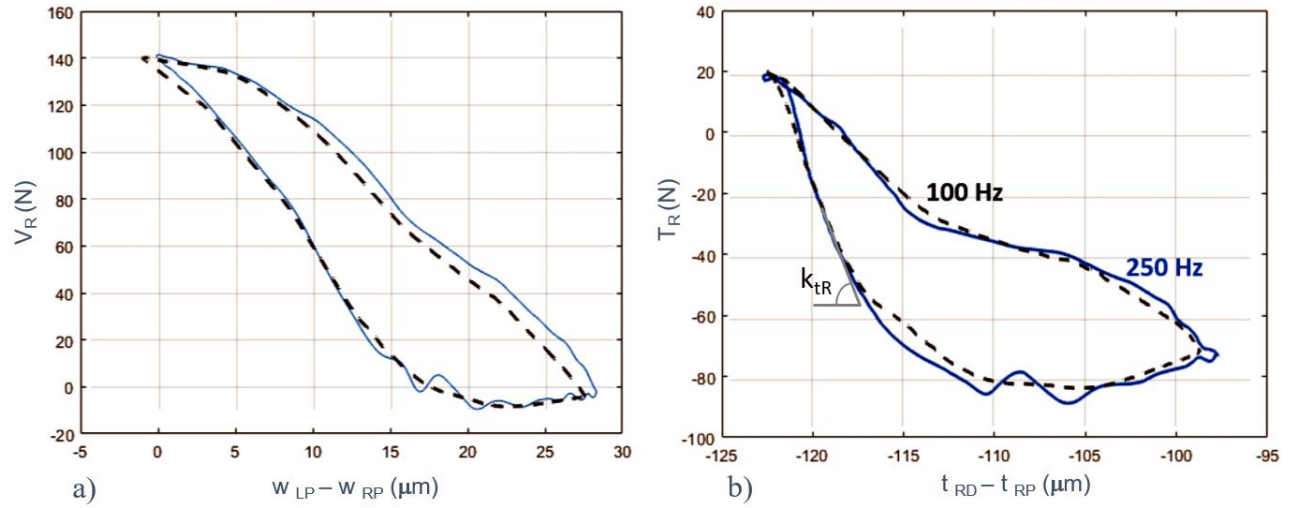

Figure 12. (a) Platform-to-platform hysteresis cycle, measured at 100 Hz (black dashed) and 250 Hz (blue solid).
(b) Right (cyl-on-flat) relative tangential displacement ds= t_{LD}-t_{LP} measured (dotted) and simulated (solid)

4. CONCLUDING REMARKS

Test rigs developed at the AERMEC lab. during slightly more than a decade have been illustrated, together with the reasons for their refinements and the related development of testing standards and procedures. These test rigs have the primary purpose to allow direct observations of contact forces exchanged between platforms and damper together with relative displacements at the damper-platform contacts in addition to the customary in-plane motion of the damper,

Results show that the accuracy, achieved after several experimental improvements illustrated in the paper, is now able to produce complete measurements that are robust and accurate, and well-aimed at assessing contact parameters.

This is a necessary pre-condition to the proper determination of contact parameters whose values are necessary to feed any software which is be currently in use for studies on the dynamics of dampers coupled to turbine blades.

The examples provided show that such results, combined with the numerical twin of the platform-damper-platform mechanics produced by the test rigs, allow a clear and detailed understanding of the damper behavior through a fine examination of hysteresis cycles.

5. REFERENCES

Botto, D., Gastaldi, C., Gola, M.M., Umer, M., 2018. "An Experimental Investigation of the Dynamics of a Blade with Two Under-Platform Dampers". Journal of Engineering for Gas Turbines and Power, Vol. 140, No. 3, pp. 032504.

Firrone, C.M., 2009, "Measurement of the kinematics of two underplatform dampers with different geometry and comparison with numerical simulation", *Journal of Sound and Vibration*, Vol. 323, No.1-5, pp. 313-333.

Gastaldi, C., 2017. "Vibration control and mitigation in turbomachinery", Ph.D. Thesis, Politecnico di Torino.

Gastaldi, C., Berruti, T.M. and Gola, M.M., 2018a. "Best practices for underplatform damper designers, *Journal of Mechanical Engineering Science*, Vol. 232, No. 7, pp. 1221-1235.

Gastaldi, C., Berruti, T.M. and Gola, M.M., 2018b. "The relevance of damper pre-optimization and its effectiveness on the forced response of blades", *Journal of Engineering for Power*, Vol. 140, No. 6, pp. 062505.

Gastaldi, C. and Gola, M.M., 2015. "A random sampling strategy for tuning contact parameters of under-platform dampers". *Proceedings of ASME Turbo Expo 2015*, Vol. 7B, Paper No. GT2015-42834, pp. V07BT33A004.

Gastaldi, C. and Gola, M.M., 2016. "Pre-Optimization of Asymmetrical Underplatform Dampers". *Journal of Engineering for Gas Turbines and Power*, Vol. 139, No. 1, pp. 012504.

Gastaldi, C. and Gola, M.M., 2016. "Testing, simulating and understanding under-platform damper dynamics". *ECCOMAS Congress 2016 - Proceedings of the 7th European Congress on Computational Methods in Applied Sciences and Engineering*, Vol. 3, pp. 4599-4610.

Gastaldi, C. and Gola, M.M., 2016. "On the relevance of a microslip contact model for under-platform dampers". *International Journal of Mechanical Sciences*, Vol. 115-116, pp. 145-156.

Gastaldi, C. and Gola, M.M., 2019. "Experimental investigation on real under-platform dampers: the impact of design and manufacturing", *Proceedings of ASME Turbo Expo 2019*, Phoenix, June 17 – 21, 2019 (GT2019-91040)

Gola, M.M., Braga Dos Santos, M. and Liu, T., 2010. "Design of a new test rig to evaluate under-platform damper performance". *Proceedings of ESDA 2010 - 10th Biennial Conference on Engineering Systems Design and Analysis* . Vol. 5, pp. 85-94.

Gola, M.M., Braga Dos Santos, M. and Liu, T., 2012. "Measurement of the scatter of underplatform damper hysteresis cycle: experimental approach". *Proceedings of ASME IDETC 2012*, Vol. 1, Paper No. DETC2012-70269, pp. 359-369.

Gola, M. M. and Gastaldi, C., 2014a. "Understanding complexities in underplatform damper mechanics". *Proceedings of ASME Turbo Expo 2014*, Vol. 7A, Paper No. GT2014-25240, pp. V07AT34A002.

Gola, M. M. and Liu, T., 2014b. "A direct experimental numerical method for investigations of a laboratory underplatform damper behavior". *International Journal of Solids and Structures*, Vol. 51, No. 25-26, pp. 4245-4259.

Griffin J.H., 1980. "Friction damping of resonant stresses in gas turbine engine airfoils". *Journal of Engineering for Power*, Vol. 102, No. 2, pp. 329-333.

Hartung, A., Hackenberg, H.-P., Krack, M., Gross, J., Heinze, T., Scheidt, L.P.-V., 2019. "Rig and Engine Validation of the Nonlinear Forced Response Analysis Performed by the Tool OrAgL", *Journal of Engineering for Gas Turbines and Power*, Vol. 141, No. 2, pp. 021019.

Hüls, M., Panning-von Scheidt, L. and Wallaschek, J., 2018. "Influence of Geometric Design Parameters Onto Vibratory Response and HCF Safety for Turbine Blades With Friction Damper". *Proceedings of ASME Turbo Expo 2018*, Vol. 7C, Paper No. GT2018-75363, pp. V07CT35A008.

Li, D., Xu, C., Liu, T., Gola, M.M. and Wen, L., 2019. "A modified IWAN model for micro-slip in the context of dampers for turbine blade dynamics", *Mechanical Systems and Signal Processing*, Vol. 121, pp. 14-30.

Liu, T., 2013, "Investigation of under-platform damper kinematics and dynamics", Ph.D. Thesis, Politecnico di Torino.

Pesaresi, L., Salles L., Jones, A., Green, J.S. and Schwingshackl, C.W., 2017. "Modelling the nonlinear behaviour of an underplatform damper test rig for turbine applications". *Mech Sys Sign Proc*, Vol. 85, pp. 662-679.

Petrov, E.P., 2018. "Stability analysis of multiharmonic nonlinear vibrations for large models of gas turbine engine structures with friction and gaps", *Journal of Engineering for Gas Turbines and Power*, Vol. 139, No. 2, pp. 022508.

6. RESPONSIBILITY NOTICE

The authors are the only responsible for the printed material included in this paper.